Available online at www.sciencedirect.com
SCIENCE DIRECT
Tetrahedron 62 (2006) 7180–7190
Tetrahedron

Structural and stereochemical aspects of the enantioselective halogenation of 1,3-dicarbonyl compounds catalyzed by Ti(TADDOLato) complexes

Mauro Perseghini, Massimo Massaccesi, Yanyun Liu and Antonio Togni*

Department of Chemistry and Applied Biosciences, Swiss Federal Institute of Technology, ETH Zürich, 8093-Zürich, Switzerland

Received 3 December 2005; accepted 5 December 2005
Available online 11 May 2006

Abstract—Complexes of the type [Ti(1-Np-TADDOLato)(carbonylenolato)$_2$] (**3a–d**), derived from β-keto esters, have been prepared and structurally characterized by NMR and X-ray crystallography. In solution, two main diastereoisomeric forms were identified. In the major C_2-symmetric isomer, the *face-on* naphthyl group of the (*S*,*S*)-TADDOL shields the *Si*-side of the coordinated enolate. Therefore, electrophilic attack of the halogenating agent can only occur at the *Re*-side of the substrate. α-Acyl-γ-lactams (**4**) were fluorinated with NFSI in the presence of the Ti(TADDOLato) catalyst in up to 87% ee. The absolute configuration of one of the products was determined by X-ray crystallography after derivatization. The observed absolute configuration at the fluorinated stereogenic center matches the one inferred from the structural analysis of the Ti(TADDOLato) complexes.

1. Introduction

We reported in 2000 the first catalytic enantioselective electrophilic fluorination of β-keto esters by Selectfluor® (1-chloromethyl-4-fluoro-1,4-diazoniabicyclo[2,2,2]octane bis(tetrafluoroborate)) in the presence of catalytic amounts of $TiCl_2$(TADDOLato) complexes.[1] Meanwhile, the field of catalytic stereoselective halogenation chemistry has become a hot topic with fundamental and innovating contributions coming from several research groups. Thus, titanium is not the only metal able to catalyze electrophilic halogenation. Pd, Ni, and Cu have been added to the list of successful systems comprising also phase-transfer and most recently organocatalytic methods (recent examples of published work are given in the references).[2–8] This frontier of asymmetric catalysis already counts several review articles, thus demonstrating the great interest by the synthetic community.[9–12]

Our first report not only had the privilege to open this new area, but at the same time constituted an important addition to the already broad spectrum of transformations for which the TADDOL ligands (α,α,α′,α′-tetraaryl-2,2-dimethyl-1,3-dioxolan-4,5-dimethanol) play a crucial role.[13,14] Subsequently, we extended this type of electrophilic atom-transfer reaction to the related chlorination and bromination,[15] a geminal dihalogenation,[16] a direct hydroxylation,[17] and most recently the first transition-metal-catalyzed sulfenylation reactions (Scheme 1).[18] It is noteworthy that for all these transformations involving a 1,3-dicarbonyl compound, the most selective catalyst contains a TADDOL bearing 1-naphthyl groups, all other ligands tested gave much lower enantioselectivities. Moreover, for a given substrate, the level of enantioselectivity is comparable for different reactions, giving rise to the conjecture that these are mechanistically related and share common intermediates. The first and simple mechanistic view of these reactions involves the coordination of the substrate to titanium in a chelating fashion and its deprotonation, followed by the external attack by the electrophile. Starting from such a hypothesis, we performed QM/MM studies of the fluorination reaction whose results are represented in Scheme 2.[19] There are two key features derived from the calculations. The first one is that the C–F bond-forming step involves a single electron transfer (SET), a characteristic that is not too surprising in view of the oxidizing properties of N–F reagents such as Selectfluor, in general. However, we were so far not able to provide experimental corroboration for the SET feature. The second important aspect that was revealed by the calculations concerns the structure of the intermediates and the specific role of the 1-naphthyl substituents on the chiral ligand in determining the stereochemical course of the reaction. We therefore decided to prepare and study Ti(enolato)

Keywords: Catalytic fluorination; Ti(TADDOLato) complexes; α-Acyl-γ-lactams; Absolute configuration.
* Corresponding author. Tel.: +41 44 6322236; fax: +41 44 6321310; e-mail: togni@inorg.chem.ethz.ch

0040–4020/$ - see front matter © 2006 Elsevier Ltd. All rights reserved.
doi:10.1016/j.tet.2005.12.071

complexes derived from selected substrates used in the catalytic reactions. We also extended the applicability of the original fluorination reaction to 3-acyl lactams. The determination of the absolute configuration of one of the products, combined with the structural analysis of the complexes, concur in providing a clear picture as to the origin of enantioselectivity, not only for the fluorination, but also for all other related reactions.

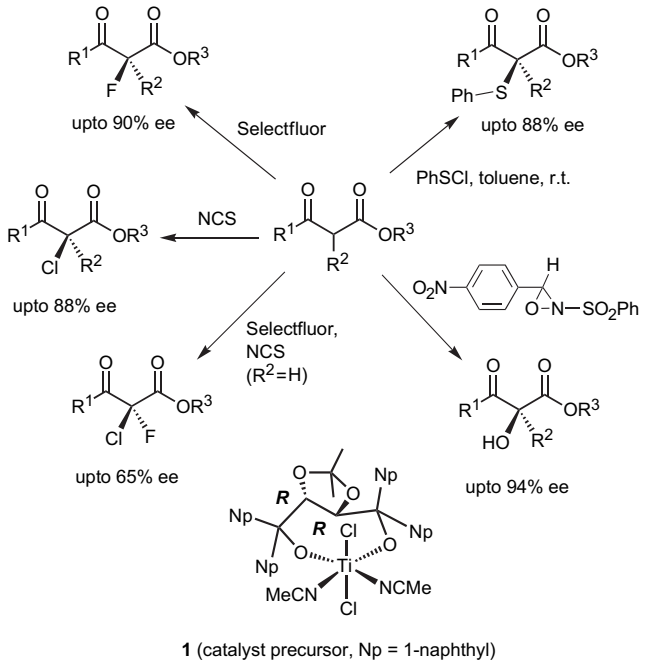

Scheme 1. Electrophilic atom-transfer reactions catalyzed by complex **1**.

2. Synthesis of Ti(enolato) complexes

In contrast to the broad range of applications, only few examples of isolated and structurally characterized TADDOLato complexes are known.[20–30] This is possibly related to the fact that in most cases the catalysts are generated in situ. On the other hand, many crystal structures of free TADDOL ligands are known, providing insights into their common structural characteristics.[28]

The catalyst precursors used in our studies are air-stable complexes of the type [Ti(TADDOLato)Cl_2L_2], whose structures have been determined by X-ray crystallography.[31] Such complexes constitute ideal starting materials for the preparation of possible intermediates generated during the catalytic reaction. First attempts have been directed at the preparation of complexes such as those postulated in the mechanistic scheme used for the above-mentioned calculations, i.e., derivatives characterized by a 1:1 ratio of metal and enolized substrate. However, we found that by reacting equivalent amounts of the catalyst precursor **1** and a Na or Li enolate of selected β-keto esters did not afford the desired compounds of type **2** (Scheme 2), but the corresponding 1:2 adducts in low yield instead, along with several side-products, as verified by NMR spectroscopy. This does not necessarily imply that the former species cannot be formed during catalysis since the reaction conditions are different for the two processes, acidic for the catalysis and basic in the case of the complex preparation. Therefore, we decided to pursue the characterization of the 1:2 adducts, convinced that a structural study of such species would in any case provide useful information in view of judging stereochemical aspects important also for the 1:1 adducts. Thus, complexes of the type [Ti(1-Np-TADDOLato)(carbonylenolato)$_2$], **3**, were obtained by reacting the catalyst precursor **1** with

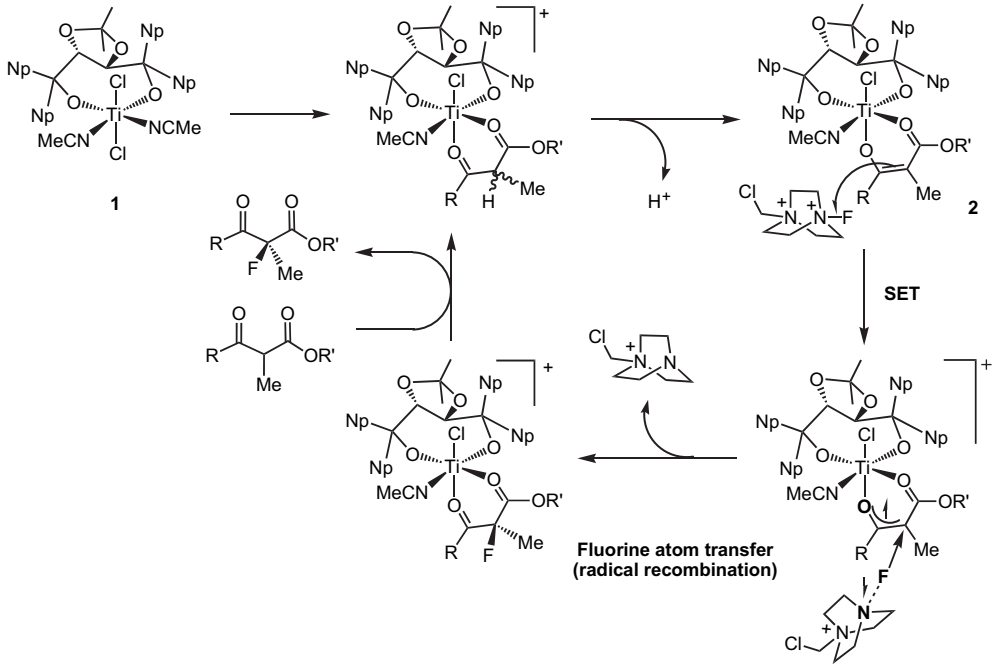

Scheme 2. Mechanistic scheme for the Ti-catalyzed fluorination of β-keto esters involving the formation of a Ti(carbonylenolato) intermediate undergoing SET with the fluorinating agent.

2 equiv of sodium enolate in benzene in up to quantitative yield (Scheme 3).

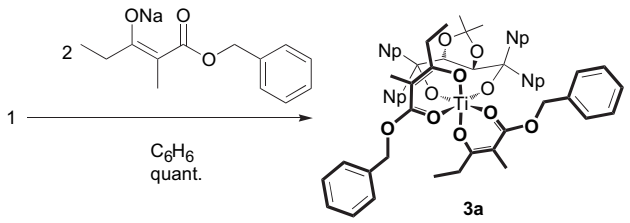

Scheme 3. The formation of complex **3a**.

Complex **3a**, containing the enolate of 2-methyl-3-oxopentanoic acid benzyl ester, is a bright yellow powder slightly soluble in chlorinated solvents (deutero chloroform and methylene chloride), where a slow decomposition is observed, and in acetonitrile. Its solubility is higher in THF, benzene, and toluene. If a solution is left in contact with air, a slow decomposition is observed by NMR after 2 days. Its stability, though, is further demonstrated by the fact that in the presence of deoxygenated water only traces of decomposition can be observed after hours. Complex **3a** did not react with an ethereal solution of HCl nor with anionic ligands such as lithium *N*,*N*′-bis(trimethylsilyl)-benzamidinate,[32] thus confirming its stability. In view of comparing structural and reactivity features, we also prepared derivatives **3b–d** by a similar procedure, containing different carbonylenolato ligands as shown in Scheme 4. The four chosen β-keto esters afford in the catalytic fluorination reaction with Selectfluor enantioselectivities between 45% and 90% ee.

3. NMR characterization of complexes 3

For complexes of type **3**, there are six possible configurational isomers, assuming a rigid conformation of the TADDOL ligand, as illustrated in Scheme 5. There are four C_2-symmetric configurations in which both carbonylenolato units show the same enantioface being shielded either by a *face-on* or an *edge-on* naphthyl group. On the other hand, in the two C_1-symmetric configurations opposite enantiofaces are shielded.

Examination of the 500 MHz ^{1}H NMR spectra of complex **3a** indicated the presence of several different species. As it will be explained below, the signal of the hydrogen atom in position 2 of a *face-on*-oriented naphthyl group appears as a doublet at relatively low field. Inspection of the spectral region between ca. 9.6 and 10 ppm allows to determine the number and relative concentration of the different isomers present in solution just by counting and integrating those signals (Fig. 1). Thus, two major isomers of **3a** in a ratio of ca. 70:30 can be identified, the major one of which is C_2-symmetric, whereas the second most abundant is not. Moreover, the ^{1}H NMR spectra reveal the presence of up to four further isomers, the concentration of which is however too low for an unambiguous identification. ^{13}C NMR measurements corroborate the observation made by ^{1}H NMR.

In order to determine the configuration and conformation of the two most abundant isomers, all corresponding proton and carbon signals for the first form, as well as relevant signals of the second form, respectively, were assigned by 2D NMR techniques. C,H-long-range correlation experiments have proven very useful for the assignment of the proton and carbon signals of the naphthyl groups. In fact, the signals of the protons in position 2 could be easily identified via their $^3J_{CH}$ correlations with the alcoholato carbon. One key point for the whole assignment is that only for the quaternary carbon atoms in position 8a of the naphthyl group there are four possible $^3J_{CH}$ interactions. Complementary H,H-COSY and TOCSY experiments confirmed the information obtained with the long-range experiment and allowed to complete the assignment. NOESY experiments delivered the necessary information to distinguish between the *face-on*- and the *edge-on*-oriented naphthyl substituents, thus determining the conformation of the TADDOLato ligand in the

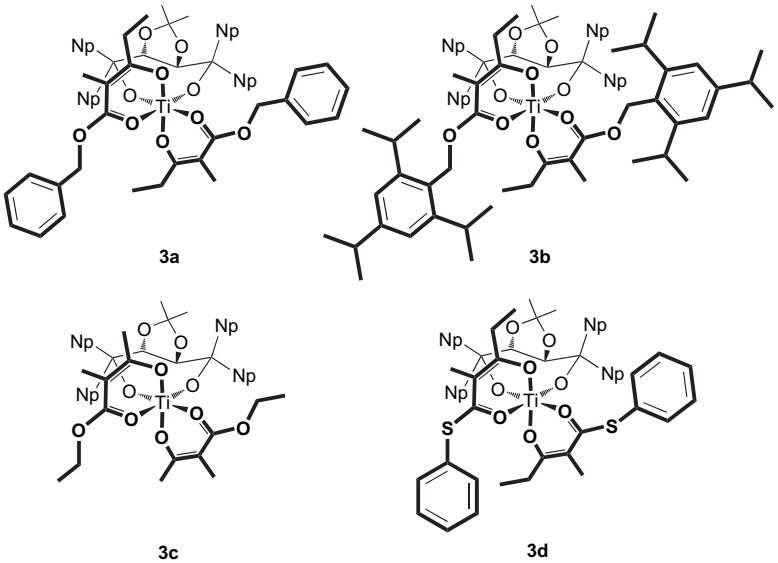

Scheme 4. The four complexes of the type [Ti(1-Np-TADDOLato)(carbonylenolato)$_2$] prepared in this work.

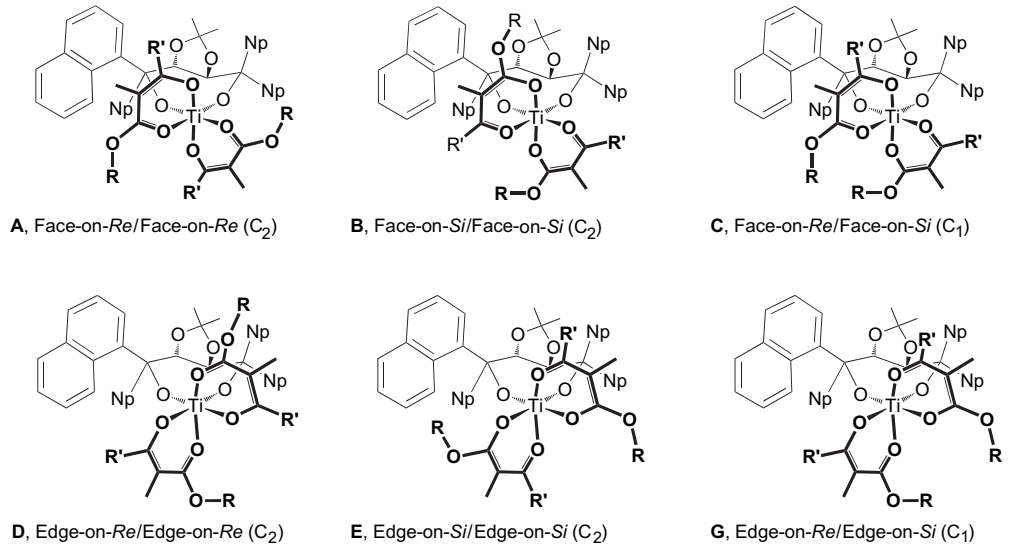

Scheme 5. The six possible diastereoisomeric forms for complexes of the type [Ti(1-Np-TADDOLato)(carbonylenolato)$_2$], assuming a rigid conformation for the TADDOL ligand (the *R*,*R*-configuration of the ligand is represented).

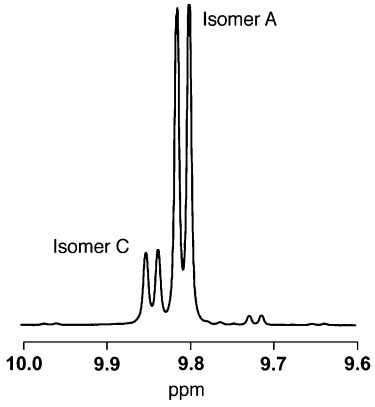

Figure 1. Section of the ^{1}H NMR spectrum (500 MHz, C_6D_6) of complex **3a** showing the signals of the hydrogen atoms in position 2 of an *edge-on* naphthyl group.

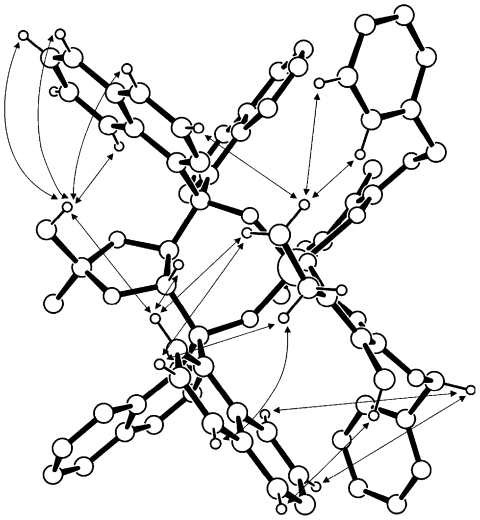

Figure 2. Selected NOEs observed for the major configuration of complex **3a**.

coordination sphere of the metal. In the next step, the NOE contacts between aromatic and aliphatic protons of the TADDOLato and carbonylenolato ligands were examined. Several NOE contacts between the protons of the *face-on* naphthyl groups and those of the carbonylenolato units allowed the determination of their relative position (Fig. 2). Furthermore, in the case of the C_2-symmetric structure **A**, contacts between aliphatic and aromatic protons of the two carbonylenolato units were observed ('head–tail' interactions).

In order to discern conformational aspects of the second most abundant form, several signals had to be assigned to the corresponding protons in the NMR spectrum. However, a complete assignment was not possible due to overlapping signals. Again, long-range interactions between protons in position 2 and the alcoholato carbons allowed the pairwise assignment of the four nonequivalent naphthyl groups to their corresponding alcoholato carbons. The *face-on* and *edge-on* substituents were then identified by NOE contacts between protons in position 2 and the H–(C) fragment of the dioxolane ring. NOE contacts between a terminal carbonylenolato H_3–(C) group and an *edge-on* naphthyl, combined with several contacts between naphthyl substituents and carbonylenolato units—as in the major form—led to the conclusion that the configuration of this form differs from that of the major form by a carbonylenolato ligand being turned by 180°, thus corresponding to isomer **C** in Scheme 5.

A first examination of the ^{1}H NMR spectra of derivatives **3b**,**c** indicated the presence of several forms, the most abundant being C_2-symmetric and accompanied by a second C_1-symmetric form, in a ratio of ca. 2:1 in both cases. The signal distribution was found to be very similar to that of complex **3a** and the subsequent 2D NMR studies confirmed configurations **A** and **C**, respectively. For complex **3d**, two isomers in a ratio of 70:30 could be identified, however, both displaying C_2-symmetry. For the major isomer, the configuration **A**

could be established again by 2D NMR methods. The determination of the configuration of the second most abundant form was complicated by overlapping signals of the thiophenyl group and some naphthyl protons which could not be assigned. However, the observation of NOE contacts between the protons of the alkanoyl group of the carbonylenolato ligand and those of both nonequivalent naphthyl groups suggests **E** as most probable configuration, i.e., both carbonylenolato ligands are shielded by *edge-on* naphthyl groups.

4. Crystal structure of complex 3a

Suitable crystals of complex **3a** (containing the *S*,*S*-configured TADDOL ligand) were grown from a mixture of THF and acetonitrile at −20 °C. Only configuration **A**—the major one observed in solution—is present in the solid state lying on a crystallographic C_2-symmetry axis, thus reducing the number of independent coordinates. The solid-state structure confirms the results obtained from the studies in solution, and clearly establishes the almost perfectly parallel orientation of the *face-on* naphthyl groups to their respective carbonylenolato units (Fig. 3).

The octahedral coordination geometry of **3a** is distorted, as shown, e.g., by the O–Ti–O angle for the apical oxygen donors derived from the keto functions of 163.46(9)°, whereas the corresponding angle for equatorially arranged ligands of 172.31(7)° is closer to the ideal value of 180° (the Ti atom and the two TADDOL oxygen atoms define the equatorial plane). Additional and probably related deviations from the usual values are found in the two O–C–C angles of the carbonylenolato chelate rings of 127.0(2)° and 123.3(2)° for the ester and keto function, respectively. The Ti–O bond length for the TADDOLato ligand atoms is 1.8006(13) Å, whereas for the carbonylenolato units the corresponding bond distances are 2.0874(15) and 1.9507(14) Å for the ester and keto function, respectively.

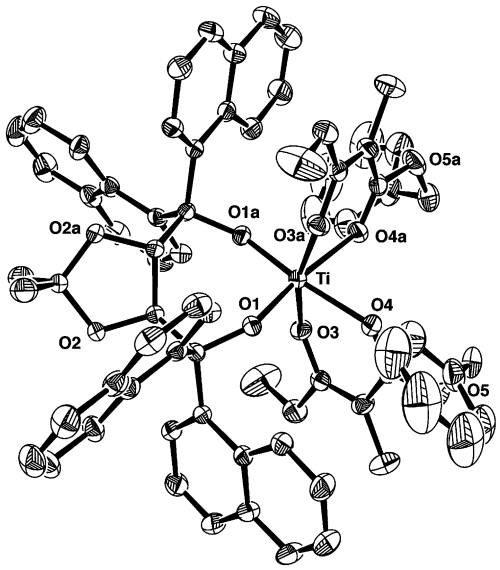

Figure 3. ORTEP drawing of the crystal structure of complex **3a**. Ellipsoids at the 30% probability level.

The least-square planes defined by the *face-on* naphthyl groups and their respective carbonylenolato chelate units are nearly parallel and form an angle of 5.68(6)°. The distances of the naphthyl carbon atoms from the carbonylenolato plane are found in the range 3.5134(22)–3.8768(26) Å, which corresponds to typical aromatic stacking distances (Fig. 4). Thus, the steric shielding of the *Si*-face of the carbonylenolato fragment by the *face-on* naphthyl substituent of the *S*,*S*-configured TADDOL ligand is virtually ideal and only the carbonylenolato *Re*-face is accessible.

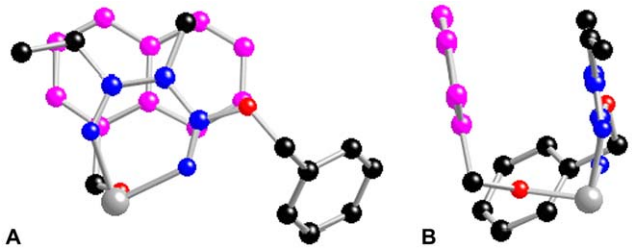

Figure 4. Partial representation of the crystal structure of complex (*S*,*S*)-**3a**, showing the shielding of the *Si*-enantioface of the carbonylenolato ligand (atoms forming the chelate ring in blue) by the *face-on* naphthyl substituent (in pink). (A) Projection on the plane of the naphthyl group; (B) side view.

5. Stoichiometric fluorination of complexes 3

In addition to the stability and reactivity experiments described above for derivative **3a**, we also performed stoichiometric fluorinations of the isomeric mixtures of the complexes. In all cases, the same preferred enantiomeric form of the products was formed as in the catalytic reaction. The fluorinated β-ketoester obtained from complex **3a** displayed an ee of 78%, slightly higher than the one obtained in the catalytic reaction using catalyst **1** (73% ee). For complexes **3b**,**c**, the enantiomeric excesses obtained were comparable to those of the catalytic reaction (90% and 77% vs 90% and 73%, respectively). For complex **3d**, a slightly lower value was observed (83% vs 90%). Furthermore, we also verified that complex **3a** can be used as a catalyst precursor and found that the corresponding enantioselectivities are close—but not identical—to those obtained with catalyst **1**. This was also the case when a mixture of two different β-keto esters (those contained in complexes **3c** and **3d**) was fluorinated using Selectfluor and catalyst **1**. These experiments do not prove the occurrence of intermediates of type **3** in the catalytic cycle, but they do not exclude it either.

6. Fluorination and derivatization of α-acyl-γ-lactams

We addressed a class of dicarbonyl compounds that have not been fluorinated previously, the α-acyl-γ-lactams. Due to their structure and versatile functional groups, α-acyl-γ-lactams appear extremely interesting and may act as valuable building blocks for the synthesis of molecules with potentially useful biological activity. Thus, 3-acetyl-1-benzyl-2-pyrrolidinone (**4a**) was recently chosen as starting material for the preparation of novel β-lactam antibiotics.[33] The methyne hydrogen of the molecule remained unaffected throughout that synthesis, hence its initial replacement

with fluorine should lead to analogous bioactive target compounds.

We therefore started our investigation with compound **4a** and tested the previously reported fluorination protocol by using Selectfluor as the fluorinating agent and our standard catalyst **1**.[1,31] Substrate **4a** was rapidly fluorinated in α-position, albeit in very modest enantioselectivity of 5% ee as determined by chiral GC (Supelco β-dex column). The competing uncatalyzed process causes lowering of the level of enantioselectivity. Therefore, the use of milder and slow reacting fluorine sources,[34] such as 1-fluoro-2,4,6-trimethylpyridinium tetrafluoroborate or *N*-fluorobenzenesulfonimide (NFSI), resulted in better values of enantiomeric excess (20% and 26% ee, respectively).

We subsequently focused on other α-acyl lactams, prepared by simple Claisen condensation reactions. The catalytic asymmetric fluorination was performed with NFSI in toluene at 0 °C, with 5 mol % of the Ti(TADDOLato) catalyst (Scheme 6). The results reported in Table 1 show that all substrates were successfully fluorinated in good yields. The enantioselectivities, ranging from scarce to good, were in all cases superior to those obtained with the fluorinating agents previously considered. This would indicate that the 'F$^+$'-donating species, in this case NFSI, plays an important role during the enantiodifferentiating step of the reaction. We took into account the influence of the R^1 and R^2 groups on the enantioselectivity. The couple of lactams **4c** (R^1=Ph, R^2=Me) and **4d** (R^1=Me, R^2=Ph) provided the lowest and the best ee values, respectively (6% and 87%). Unexpectedly, though, reciprocally exchanging the positions of the cyclohexyl and methyl group, as in the substrates **4e** and **4f** (entries 5 and 6), resulted in the same level of asymmetric induction (50% and 46% ee, respectively). These observations indicate that the enantioselectivity of the fluorination reaction is influenced not only by the steric bulk of the substituents R^1 and R^2, but also by their electronic nature. In the fluorination of the substrates **4d** and **4f**, in which the two relatively bulky R^2 groups (Ph and Cy, respectively) are clearly different electronically, we observed a marked difference in enantioselectivity.

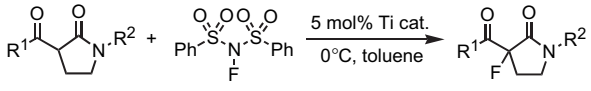

4 5

Scheme 6. Catalytic fluorination of α-acyl-γ-lactams.

Table 1. Fluorination of α-acyl-γ-lactams with NFSI catalyzed by (*S*,*S*)-**1**

Entry	Substrate	R^1	R^2	Yield[a] (%)	ee[b] (%)
1	**4a**	Me	CH_2Ph	75	26
2	**4b**	Ph	CH_2Ph	78	15
3	**4c**	Ph	Me	75	6
4	**4d**	Me	Ph	75	87
5	**4e**	Cy	Me	60	50
6	**4f**	Me	Cy	n/d	46
7	**4g**	*t*-Bu	Me	40	20

[a] Yields refer to isolated products.
[b] The absolute configuration *R* of the major enantiomer has been determined in the case of **5d** (vide infra).

Since the fluorinated products **5** are new compounds, it was important to determine the absolute configuration at least in one case, thus allowing to draw conclusions as to the sense of chiral induction. To this purpose, the enantiomerically enriched product **5d**, obtained upon fluorination with NFSI using (*S*,*S*)-**1** as a catalyst, was subjected to reduction by transfer hydrogenation using Noyori's Ru catalyst in isopropanol.[35] The α-(1-hydroxyalkyl)-γ-lactam **6d**, which is a mixture of two diastereoisomeric pairs of enantiomers, was subjected to column chromatographic purification. The major fraction was subsequently derivatized with *S*-camphorsulfonyl chloride affording **7** (Scheme 7). Derivative **7** turned out to be a crystalline material and crystals suited for an X-ray diffraction study were grown from a CD_2Cl_2 solution overlaid with hexane in an NMR tube. The solid-state structure of **7** allowed the determination of the absolute configuration of the two stereogenic centers generated in the two catalytic reactions, by internal comparison. The structure is illustrated in Figure 5 and clearly shows that the C–F stereogenic center has *R* absolute configuration and that, therefore, the fluorine atom has been delivered to the *Re*-enantioface of the corresponding enolate precursor while coordinated to Ti, as was to be expected for catalyst (*S*,*S*)-**1**, based on the consideration made above.

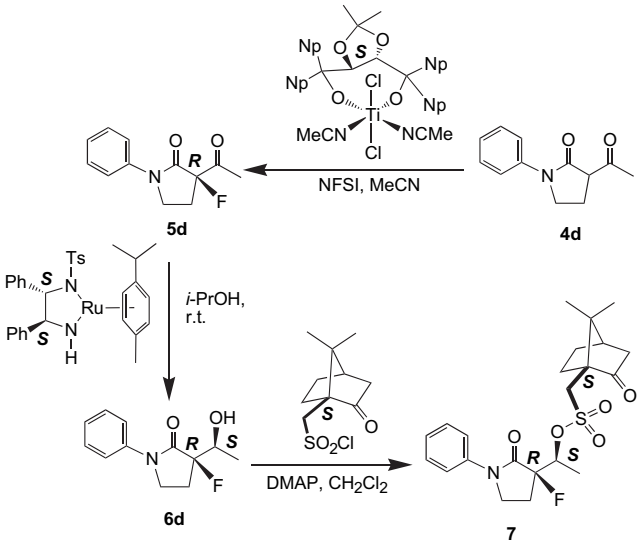

Scheme 7. Fluorination, reduction, and derivatization of α-acyl-γ-lactam **4d**.

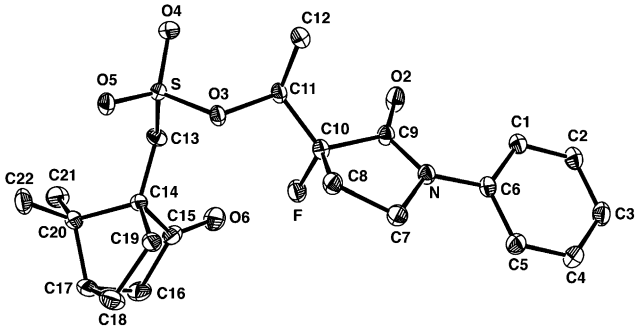

Figure 5. ORTEP drawing of the crystal structure of compound **7**. Ellipsoids at the 30% probability level.

7. Conclusion

The conformation and configuration of four Ti (TADDOLato) complexes bearing two carbonylenolato units (**3a**–**d**) have been determined in solution by 2D NMR methods. These materials consist of a mixture of up to six possible diastereoisomeric forms, two of which account for more than 90% of the mixture in all cases studied. The 1-naphthyl substituents of the TADDOL ligand are pairwise arranged in a *face-on* and *edge-on* orientation, respectively,[13] corresponding to a rigid conformation on the NMR timescale. The *face-on* naphthyl groups are responsible for an ideal steric shielding of one face of any bidentate chelating ligand occupying one equatorial and one apical position in a corresponding octahedral complex. This is clearly shown by the solid-state structure of derivative **3a**, the major species found in solution for this complex. Thus, in this steric shielding of one enantioface of the coordinated carbonylenolato ligand lies the origin of enantioselectivity of the Ti(TADDOLato) system in electrophilic atom-transfer reactions to 1,3-dicarbonyl compounds. However, the existence of isomeric forms of complexes containing both one or two carbonylenolato units, differing by the enantioface being shielded, explains why the enantioselectivities obtained with this system rarely go beyond ca. 90% ee. In other words, the observed enantioselectivity is the result of several factors, such as the isomeric composition of Ti(carbonylenolato) adducts, the relative rates by which they undergo atom-transfer reactions, their interconversion, and the degree of discrimination of the substrate enantiofaces when comparing *face-on* and *edge-on* shielding. Nevertheless, we can reduce the problem of enantioselectivity to a large extent to the problem of controlling the formation of the diastereoisomeric intermediates. Since the steric influence of the two ends of the substrate molecules does not let recognize clear trends, one should seek the solution to the problem in electronic factors, more specifically. How can the preference for the arrangement of the enolate and the carbonyl donor atoms in axial and equatorial position, respectively, be further enhanced? How should the TADDOL ligand be modified in order to achieve such an improved differentiation? We are currently working at these problems and shall deliver answers in due course.

8. Experimental

8.1. General

Reactions were carried out under argon (Schlenk) or under nitrogen atmosphere (glovebox). Freshly distilled solvents were used throughout. Organic solvents were purified by standard procedures. ^{1}H, $^{13}C\{^{1}H\}$ NMR, and 2D NMR spectra were recorded with Bruker DPX-300 or DRX-500 spectrometers using standard pulse sequences. ^{1}H and ^{13}C chemical shifts are relative to tetramethylsilane and calibrated against solvent resonance. Coupling constants are given in Hz. In the assignment of naphthyl resonances for complexes **3**, A refers to *face-on* and B to *edge-on* groups, for C_2-symmetric forms. For C_1-symmetric forms, A and D are *face-on* and B and C are *edge-on* groups. Infrared spectra were recorded on Perkin–Elmer FT-IR Paragon 1000 spectrometers. Mass spectrometry was carried out by the Analytical Service of the Organic Chemistry Laboratory, ETH Zürich. Microanalysis was performed by the Microelemental Analysis Service of the Organic Chemistry Laboratory, ETH Zürich.

Crystallographic data (excluding structure factors) for the structures in this paper have been deposited with the Cambridge Crystallographic Data Center as supplementary publication numbers CCDC-208619 (**3a**) and CCDC-251473 (**7**). Copies of the data can be obtained, free of charge, on application to CCDC, 12 Union Road, Cambridge CB2 1EZ, UK [fax: +44-(0)1223-336033 or e-mail: deposit@ccdc.cam.ac.uk].

8.2. Titanium complex 3a

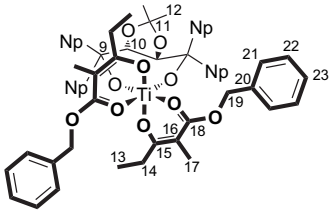

The precursor **1** was freshly prepared from 200 mg (300 μmol) 1-Np-TADDOL and 71.5 mg (302 μmol) $TiCl_2(O^iPr)_2$ in 4 ml MeCN. After stirring for 2 h, a white precipitate formed. The solvent was removed (HV), the light yellow residue dried (16 h, HV) and then dissolved in 10 ml benzene. To a suspension of 14.6 mg (608 μmol) sodium hydride in 6 ml benzene, 132.4 mg (601 μmol) benzyl 2-methyl-3-oxo-pentanoate was added. When gas evolution ceased (30 min), the suspension was added to the solution of complex **1**. After standing (2.5 h), the NaCl precipitate was removed by filtration and the obtained yellow solution was dried (HV). The yellow residue was dissolved in 2 ml benzene. Addition of 10 ml pentane caused the precipitation of a light yellow solid, which was separated, washed (3×4 ml pentane), and dried (HV) to give the product as light yellow powder (395 mg, quant.). Found: C, 76.16; H, 5.97. $C_{73}H_{66}O_{10}Ti$ (1151.20) requires: C, 76.16; H, 5.78. Major isomer: δ_H (500 MHz, C_6D_6): 0.13 (s, H–C(12)), 1.07 (s, H–C(17)), 1.40 (t, J=7.5, H–C(13)), 1.79 (dq, J=15.4, 7.5 H–C_{out}(14)), 2.09 (dq, J=15.4, 7.5, H–C_{in}(14)), 4.66 (d, J=12.0, H–C(19)), 4.86 (d, J=12.0, H–C(19)), 6.42 (dd, J=8.9, 7.2, H–C(7A)), 6.71 (s, H–C(10)), 6.73 (t, J=7.9, H–C(7B)), 6.85 (t, J=7.5, H–C(6B)), 6.88 (t, J=7.2, H–C(6A)), 6.94 (t, J=7.4, H–C(23)), 7.02 (t, J=7.4, H–C(22)), 7.13 (d, J=7.4, H–C(21)), 7.38 (dd, J=8.1, 7.5, H–C(3A)), 7.43 (d, J=8.1, H–C(5A)), 7.48 (d, J=8.1, H–C(5B)), 7.58 (d, J=8.1, H–C(4A)), 7.81 (d, J=8.0, H–C(4B)), 8.00 (dd, J=8.0, 7.5, H–C(3B)), 8.18 (d, J=9.1, H–C(8B)), 8.48 (d, J=8.9, H–C(8A)), 8.74 (d, J=7.5, H–C(2A)), 9.81 (dd, J=7.5, 1.2, H–C(2B)). δ_C (75.5 MHz, C_6D_6): 10.4 (C(13)), 11.2 (C(17)), 27.2 (C(12)), 29.1 (C(14)), 66.9 (C(19)), 83.1 (C(10)), 94.2 (C(16)), 97.1 (C(9)), 112.5 (C(11)), 124.3 (C(7B)), 124.8 (C(2A)), 124.8 (C(6B)), 124.9 (C(3A)), 124.9 (C(7A)), 125.0 (C(3B)), 125.1 (C(6A)), 127.7 (C(8A)), 128.2 (C(5A)), 128.2 (C(23)), 128.3 (C(5B)),

128.4 (C(2B)), 128.4 (C(22)), 128.7 (C(8B)), 128.9 (C(4A)), 129.3 (C(21)), 129.4 (C(4B)), 132.8 (C(8aA)), 134.1 (C(8aB)), 134.9 (C(4aB)), 135.0 (C(4aA)), 136.6 (C(20)), 142.5 (C(1B)), 144.5 (C(1A)), 171.5 (C(18)), 184.7 (C(15)). ν_{max} (cm^{-1}, KBr pellet): 3047m, 2981m, 2933m, 1625s, 1599s, 1494bs, 1452s, 1405s, 1347m, 1258bs, 1236s, 1185s, 1089s, 1047s, 970s, 889s, 801s, 779s, 699m, 644m, 518m, 467s, and 436s. *m/z* (FAB): 1152.1 (M^+). Second form (detected signals): δ_H (500 MHz, C_6D_6): 0.14 (s, H–C(12)), 0.29 (s, H–C(12)), 0.92 (t, *J*=7.7, H–C(13)), 1.14 (s, H–C(17)), 1.22 (s, H–C(17)), 1.47 (t, *J*=7.6, H–C(13)), 1.79 (H–C(14)), 1.89 (m, H–C(14)), 1.96 (m, H–C(14)), 2.15 (m, H–C(14)), 4.38 (d, *J*=12.4, H–C(19)), 4.85 (d, *J*=12.1, H–C(19)), 4.87 (d, *J*=12.1, H–C(19)), 4.97 (d, *J*=12.4, H–C(19)), 6.28 (t, *J*=7.7, H–C(7A)), 6.47 (t, *J*=7.8, H–C(7C)), 6.66 (d, *J*=6.1, H–C(10B)), 6.86, 6.86, 6.73, 6.92, 7.19 (H–C(10A)), 7.19, 7.25 (t, *J*=7.8, H–C(4A)), 7.30 (H–C(2C)), 7.30 (H–C(3D)), 7.40, 7.49, 7.57 (H–C(3A)), 7.57 (H–C(4D)), 7.88, 8.10 (d, *J*=9.1), 8.36 (d, *J*=8.8), 8.42 (d, *J*=7.3, C(2A)), 8.55 (d, *J*=7.5, H–C(2D)), 8.62 (d, *J*=7.2, H–C(8D)), 9.85 (d, *J*=7.3, H–C(2B)), 10.88 (d, *J*=8.8). δ_C (75.5 MHz, C_6D_6): 10.9, 11.3, 11.4, 11.5 (13, 13, 17, 17), 27.3 (C(12)), 28.2 (C(12)), 29.5 (C(14)), 29.5 (C(14)), 66.7 (C(19)), 66.7 (C(19)), 83.5 (C(10B)), 84.0 (C(10A)), 93.7 (C(16)), 94.7 (C(16)), 97.6 (C(9A)), 101.5 (C(9B)), 113.2 (C(11)), 123.5, 124.0, 124.6 (C(2D)), 125.2 (C(2A)), 127.9, 128.0 (C(2B)), 126.3, 128.7, 129.0 (C(21)), 129.3 (C(8D)), 129.7, 132.2 (C(2C)), 132.7 (C(8aA)), 134.3, 135.3, 135.6, 138.8 (C(1C)), 142.8 (C(1B)), 144.0 (C(1A)), 146.0 (C(1D)), 171.0 (C(18)), 172.0 (C(18)), 184.2 (C(15)), 184.9 (C(15)). Third form: δ_H (500 MHz, C_6D_6): 0.70 (d, *J*=7.6), 0.77 (t, *J*=7.5), 0.88 (t, *J*=7.5), 1.36 (t, *J*=7.5), 5.49 (d, *J*=12.2), 6.00 (d, *J*=12.2), 6.58 (*m*), 7.08 (d, *J*=7.7; this signal could also arise from two overlapping triplets), 7.96 (d, *J*=7.7), 8.14 (d, *J*=9.1), 8.29 (d, *J*=9.1), 8.88 (d, *J*=7.3), 9.03 (d, *J*=7.1), 9.72 (d, *J*=7.3).

8.3. Titanium complex 3b

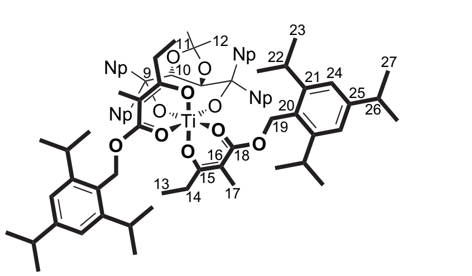

A suspension of 149.6 mg (431.7 μmol) 2,4,6-triisopropyl 2-methyl-3-oxo-pentanoate and 10.5 mg (438 μmol) sodium hydride in 6 ml toluene was stirred for 1.5 h (after 10 min a colorless solution was observed). A solution of 178.0 mg (215.9 μmol) of complex **1** was added. After 4 h without stirring, no precipitate was observed, even after reduction of the solution volume to 3 ml and cooling at −100 °C. The solvent was removed completely (HV). The light brown residue was dried (HV, 5 h), then washed three times with 8 ml pentane and dried (HV, 6 h). The complex was analyzed without further purification. δ_H (500 MHz, C_6D_6): 0.13 (H–C(12)), 1.09 (s, H–C(17)), 1.13 (d, *J*=6.8, H–C(23)), 1.15 (d, *J*=6.9, H–C(27)), 1.24 (d, *J*=6.8, H–C(23′)), 1.38 (t, *J*=7.2, H–C(13)), 1.74–1.84 (m, H–C(14)), 2.06–2.16 (m, H–C(14)), 2.72 (sept, *J*=6.9, H–C(26)), 3.29 (sept, *J*=6.8, H–C(22)), 5.04 (d, *J*=12.2, H–C(19)), 5.59 (d, *J*=12.2, H–C(19)), 6.67 (H–C(7A)), 6.73 (H–C(10)), 6.74 (H–C(7B)), 6.88 (H–C(6B)), 6.91 (H–C(6A)), 7.06 (s, H–C(24)), 7.40 (t, *J*=8.2, H–C(3A)), 7.45 (d, *J*=8.4, H–C(5A)), 7.49 (d, *J*=8.4, H–C(5B)), 7.60 (d, *J*=8.2, H–C(4A)), 7.79 (d, *J*=7.8, H–C(4B)), 7.95 (t, *J*=7.7, H–C(3B)), 8.22 (d, *J*=8.6, H–C(8B)), 8.55 (d, *J*=8.3, H–C(8A)), 8.77 (d, *J*=7.3, H–C(2A)), 9.73 (d, *J*=7.3, H–C(2B)). δ_C (75.5 MHz, C_6D_6): 10.3 (C(13)), 11.4 (C(17)), 24.1 (C(27)), 24.5 (C(23)), 24.6 (C(23′)), 27.3 (C(12)), 29.2 (C(14)), 29.7 (C(22)), 34.8 (C(26)), 59.0 (C(19)), 83.3 (C(10)), 93.7 (C(16)), 96.8 (C(9)), 112.7 (C(11)), 121.3 (C(24)), 124.3 (C(7B)), 124.8 (C(6A)), 124.9 (C(3A)), 124.9 (C(7A)), 124.9 (C(6B)), 125.1 (C(2A)), 125.1 (C(3B)), 127.6 (C(20)), 127.8 (C(8A)), 128.3 (C(5A)), 128.3 (C(2B)), 128.4 (C(5B)), 128.8 (C(8B)), 128.9 (C(4A)), 129.4 (C(4B)), 132.9 (C(8aA)), 134.2 (C(8aB)), 134.9 (C(4aB)), 135.1 (C(4aA)), 142.4 (C(1B)), 144.5 (C(1A)), 149.2 (C(21)), 149.8 (C(25)), 171.0 (C(18)), 184.4 (C(15)). ν_{max} (cm^{-1}, KBr pellet): 3047m, 2961s, 2931s, 2869m, 1627s, 1603s, 1508bs, 1459s, 1404s, 1262bs, 1232bs, 1187s, 1090bs, 1045bs, 963s, 887s, 779s, 644m, 618m, 518m.

8.4. Titanium complex 3c

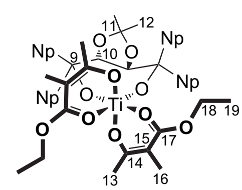

A solution of 5.0 mg (35 μmol) ethyl acetoacetate in 0.3 ml C_6D_6 was added to 1.4 mg (61 μmol) sodium hydride. After almost complete gas evolution, the suspension was added to 15.0 mg (17.3 μmol) of complex **1** and diluted to 1 ml with C_6D_6. To remove traces of uncoordinated ethyl acetoacetate, the solution was dried (HV, 1 h) and the residue washed (3×1 ml pentane), dried (HV, 3 h), and dissolved in 0.7 ml C_6D_6 for spectroscopic analyses. δ_H (500 MHz, C_6D_6): 0.12 (s, H–C(12)), 0.70 (t, *J*=7.2, H–C(19)), 0.98 (s, H–C(16)), 1.83 (s, H–C(13)), 3.53–3.61 (m, H_{out}–C(18)), 3.66–3.77 (m, H–C(18)), 6.66 (s, H–C(10)), 6.72 (H–C(7A)), 6.72 (H–C(7B)), 6.84 (H–C(6B)), 6.88 (H–C(6A)), 7.43 (H–C(5A)), 7.47 (H–C(5B)), 7.37 (t, *J*=7.8, H–C(3A)), 7.57 (H–C(4A)), 7.76 (t, *J*=8.0, H–C(4B)), 7.91 (t, *J*=8.0, H–C(3B)), 8.11 (d, *J*=8.8, H–C(8B)), 8.53 (d, *J*=9.0, H–C(8A)), 8.69 (d, *J*=7.4, H–C(2A)), 9.86 (d, *J*=7.6, H–C(2B)). δ_C (75.5 MHz, C_6D_6): 11.6 (C(16)), 13.5 (C(19)), 23.3 (C(13)), 27.1 (C(12)), 61.1 (C(18)), 95.5 (C(15)), 82.9 (C(10)), 97.1 (C(9)), 112.3 (C(11)), 124.2 (C(7B)), 124.3 (C(2A)), 124.7 (C(6B)), 124.8

(C(7A)), 124.9 (C(6A)), 125.1 (C(3A)), 125.1 (C(3B)), 127.5 (C(8A)), 128.4 (C(5A)), 128.4 (C(5B)), 128.7 (C(2B)), 128.7 (C(8B)), 128.9 (C(4A)), 129.4 (C(4B)), 132.8 (C(8aA)), 134.1 (C(8aB)), 134.8 (C(4aB)), 135.2 (C(4aA)), 143.1 (C(1B)), 144.9 (C(1A)), 172.1 (C(17)), 180.4 (C(14)). Second form (detected signals): δ_H (500 MHz, C_6D_6): 0.09 (s), 0.25 (s), 0.65 (t, J=7.2), 0.80 (7, J=7.2), 0.99 (s), 1.24 (s), 1.61 (s), 1.91 (s), 3.45–3.56 (m), 3.82–3.88 (m), 8.04 (d, J=9.0), 8.39 (d, J=7.2), 8.42 (d, J=9.0), 9.82 (d, J=7.4), 10.93 (d, J=8.4).

8.5. Titanium complex 3d

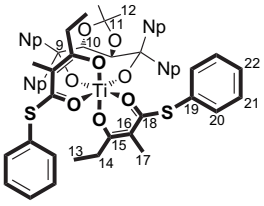

A solution of 41.5 mg (187 μmol) thiophenyl 2-methyl-3-oxo-pentanoate in 3 ml toluene was added to 4.5 mg (0.19 mmol) sodium hydride. After the gas evolution ceased, the solution was added to 80.4 mg (92.9 μmol) of complex **1** in 12 ml toluene. After standing (15 h), the yellow solution was separated from the white precipitate and dried (HV). The light yellow oil was washed (3×1 ml pentane). The resulting yellow powder was dried (HV, 4 h), affording 55 mg (53%) product. Major isomer: δ_H (500 MHz, C_6D_6): 0.06 (s, H–C(12)), 1.11 (s, H–C(17)), 1.16 (t, J=7.2, H–C(13)), 1.42–1.51 (m, H_{out}–C(14)), 1.69–1.78 (m, H_{in}–C(14)), 6.50 (s, H–C(10)), 6.72 (H–C(7B)), 6.84 (H–C(6B)), 6.99 (H–C(7A)), 7.03 (H–C(6A)), 7.34 (t, J=7.0, H–C(3A)), 7.46 (H–C(5A)), 7.46 (H–C(5B)), 7.56 (d, J=8.1, H–C(4A)), 7.71 (H–C(4B)), 7.79 (t, J=7.4, H–C(3B)), 8.19 (d, J=9.0, H–C(8B)), 8.39 (d, J=8.3, H–C(8A)), 8.64 (d, J=7.2, H–C(2A)), 9.32 (d, J=7.2, H–C(2B)). Not detected: H–C(20) to H–C(22). δ_C (126 MHz, C_6D_6): 9.2 (C(13)), 12.4 (C(17)), 27.2 (C(12)), 29.3 (C(14)), 83.2 (C(10)), 96.9 (C(9)), 104.1 (C(16)), 112.7 (C(11)), 124.8 (C(3A)), 124.8 (C(6A)), 124.3 (C(7A)), 124.7 (C(2B)), 124.8 (C(3B)), 125.4 (C(6B)), 125.8 (C(7B)), 127.8 (C(8B)), 128.0 (C(5B)), 128.1 (C(2A)), 128.3 (C(5A)), 128.7 (C(8A)), 128.8 (C(4B)), 129.4 (C(4A)), 132.7 (C(8aB)), 134.0 (C(8aA)), 134.8 (C(4aA)), 134.8 (C(4aB)), 141.9 (C(1A)), 144.3 (C(1B)), 183.5 (C(15)), 187.3 (C(18)). Not detected: C(19) to C(22). Second form (detected signals): δ_H (500 MHz, C_6D_6): 0.73 (t, J=7.4, H–C(13)), 1.17 (m, H–C(14)), 1.58 (s, H–C(17)), 1.87–1.96 (m, H–C(14)), 6.68 (H–C(7B)), 6.77 (s, H–C(10)), 6.79 (H–C(7A)), 7.74 (H–C(4)), 7.50 (H–C(3A)), 7.77 (H–C(3B)), 8.99 (d, J=7.2, H–C(2B)), 8.02 (d, J=9.0, H–C(8B)), 8.43 (d, J=8.8, H–C(8A)), 8.77 (d, J=7.3, H–C(2A)). δ_C (126 MHz, C_6D_6): 9.4 (C(13)), 13.1 (C(17)), 29.7 (C(14)), 82.3 (C(10)), 97.0 (C(9)), 105.0 (C(16)), 124.8 (C(2A)), 127.6 (C(2B)), 128.0 (C(8A)), 128.6 (C(8B)), 132.9 (C(8aA)), 134.2 (C(8aB), 134.9 (C(4aB)), 135.2 (C(4aA)), 143.0 (C(1B)), 143.7 (C(1A)), 184.5 (C(15)), 188.1 (C(18)).

8.6. Typical experimental procedure for the catalytic fluorination of α-acyl-γ-lactams

Complex **1** (0.05 mmol) was added to a solution of α-acyl-γ-lactam **4** (1 mmol) in dry toluene at room temperature. After 15 min, the mixture was cooled to 0 °C, then NFSI (1.2 mmol) was added. The reaction was monitored by TLC and GC–MS, and after completion water was added. The organic layer was extracted with TBME, dried over $MgSO_4$, and the crude product was purified by column chromatography. Spectroscopic and analytical data for selected examples follow.

8.6.1. 3-Acetyl-1-benzyl-3-fluoro-2-pyrrolidinone (5a). δ_H (200 MHz, $CDCl_3$): 2.05–2.35 (m, 1H, CH_2), 2.49 (d, 3H, CH_3, $^4J_{HF}$=5.0), 2.55–2.75 (m, 1H, CH_2), 3.25–3.45 (m, 2H, CH_2), 4.51 (s, 2H, CH_2), 7.20–7.45 (m, 5H, Ph); δ_C NMR (75 MHz, $CDCl_3$): 26.4 (CH_3), 28.6 (d, CH_2, $^2J_{CF}$=21.4), 43.0 (d, CH_2, $^3J_{CF}$=3.1), 47.2 (CH_2), 99.5 (d, C, J_{CF}=199.0), 127.9 (CH), 128.0 (CH), 128.8 (CH), 134.9 (C), 166.8 (d, C, $^2J_{CF}$=23.7), 205.7 (d, C, $^2J_{CF}$=32.3); δ_F (188 MHz, $CDCl_3$): −158.5/−158.8 (m); *m/z* (EI): 235 (M^+), 215, 192, 118, 91 (100), 65, 43. Found: C, 66.25; H, 6.21; N, 5.95. $C_{13}H_{14}NO_2F$ (235.26) requires: C, 66.37; H, 6.00; N, 5.95.

8.6.2. 3-Benzoyl-1-methyl-3-fluoro-2-pyrrolidinone (5c). δ_H (250 MHz, $CDCl_3$): 2.25–2.55 (m, 1H, CH_2), 2.85–3.00 (m, 1H, CH_2), 2.95 (s, 3H, CH_3), 3.47 (dt, 1H, CH_2, J_{HH}=9.0, J_{HH}=2.5), 3.55–3.60 (m, 1H, CH_2), 7.45–7.65 (m, 3H, Ph), 8.20–8.25 (m, 2H, Ph); δ_C (75 MHz, $CDCl_3$): 30.3 (CH_3), 30.7 (d, CH_2, $^2J_{CF}$=21.8), 45.8 (d, CH_2, $^3J_{CF}$=3.8), 100.5 (d, C, J_{CF}=202.3), 128.2 (d, CH, $^5J_{CF}$=1.1), 130.2 (d, CH, $^4J_{CF}$=6.6), 133.6 (CH), 134.0 (d, C, $^3J_{CF}$=4.3), 167.9 (d, C, $^2J_{CF}$=23.7), 196.4 (d, C, $^2J_{CF}$=29.3); δ_F (188 MHz, $CDCl_3$): −152.4 (d, C, $^3J_{HF}$=25.8); *m/z* (EI): 221 (M^+), 201, 116, 105 (100), 77, 51. Found: C, 65.13; H, 5.61; N, 6.30. $C_{12}H_{12}NO_2F$ (221.23) requires: C, 65.15; H, 5.47; N, 6.33.

8.6.3. 3-Acetyl-3-fluoro-1-phenyl-2-pyrrolidinone (5d). δ_H (200 MHz, $CDCl_3$): 2.30–2.60 (m, 1H, CH_2), 2.52 (d, 3H, CH_3, $^4J_{HF}$=4.8), 2.75–3.00 (m, 1H, CH_2), 3.85–4.10 (m, 2H, CH_2), 7.20–7.25 (m, 1H, Ph), 7.40–7.55 (m, 2H, Ph), 7.60–7.70 (m, 2H, Ph); δ_C (75 MHz, $CDCl_3$): 26.2 (CH_3), 28.2 (d, CH_2, $^2J_{CF}$=21.0), 44.8 (d, CH_2, $^3J_{CF}$=3.4), 99.6 (d, C, J_{CF}=199.7), 119.9 (CH), 125.7 (CH), 128.9 (CH), 138.1 (C), 165.6 (d, C, $^2J_{CF}$=23.7), 205.0 (d, C, $^2J_{CF}$=32.5); δ_F (188 MHz, $CDCl_3$): −157.0/−157.5 (m); *m/z* (EI): 221 (M^+), 201, 179 (100), 159, 119, 104, 77, 43. Found: C, 65.22; H, 5.71; N, 6.34. $C_{12}H_{12}NO_2F$ (221.23) requires: C, 65.15; H, 5.47; N, 6.33.

8.7. 3-Fluoro-3-(1-hydroxyethyl)-1-phenyl-2-pyrrolidinone (6d)

A sample of 3-acetyl-3-fluoro-1-phenyl-2-pyrrolidinone (**5d**, 100 mg, 0.45 mmol, 53% ee, as obtained from the fluorination of **4d** using *S*,*S*-**1** as catalyst and Selectfluor) and [Ru((1*S*,2*S*)-*p*-TsNCH(C_6H_5)CH(C_6H_5)NH)(η^6-*p*-cymene)] (2.5 mg, 0.0045 mmol, 1 mol%) in 3 ml of isopropanol was stirred under argon at room temperature for 10 h. The reaction mixture was concentrated under reduced pressure.

The residue was purified by flash chromatography on silica gel using a 1:1 hexane/TBME mixture as an eluent to afford the products (44 mg, 43.6%) and recovered starting material (43 mg). Less polar isomer of the product (14 mg, 90% ee): R_f (hexane/TBME 1:2)=0.34 (UV, $KMnO_4$). δ_H (200 MHz, $CDCl_3$): 1.31 (d, J=6.4, 3H, CH_3), 2.13–2.31 (m, 1H), 2.47–2.74 (m, 2H), 3.75–4.00 (m, 2H), 4.31 (dq, J=10, 7, 1H), 7.21 (t, J=7.4, 1H), 7.40 (t, J=8.2, 2H), 7.65 (d, J=8.0); δ_F (188.3 MHz, $CDCl_3$): δ −158.1 (dt, J=26, 6.5); HPLC conditions: Agilent 1100, Daicel Chiracel Column (250×4.6 mm) OD–H, hexane/*i*-PrOH (96:4), 1.0 ml/min, detector 210 nm, retention times 20.5 (major) and 23.0 min. More polar isomer (30 mg, 96% ee): R_f (hexane/TBME 1:2)=0.40 (UV, $KMnO_4$). δ_H (200 MHz, $CDCl_3$): 1.25 (d, J=6.4, 3H, CH_3), 2.12–2.52 (m, 2H), 3.69–3.81 (m, 2H), 3.87–3.99 (m, 2H), 4.22(dq, J=16, 7, 1H), 7.21 (t, J=7.2, 1H), 7.39 (t, J=8.0, 2H), 7.63 (d, J=8.2); δ_F (188.3 MHz, $CDCl_3$): −164.0–164.3 (m); HPLC conditions: Agilent 1100, Daicel Chiracel Column (250×4.6 mm) OD–H, hexane/*i*-PrOH (96:4), 1.0 ml/min, detector 210 nm, retention times 41.9, 43.2 (major).

8.8. Compound 7

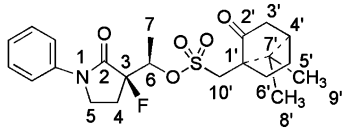

A solution of 3-fluoro-3-(1-hydroxyethyl)-1-phenyl-2-pyrrolidinone (**6d**, 30 mg, 0.13 mmol, 96% ee) and DMAP (22.6 mg, 0.2 mmol, 1.5 equiv) in 2 ml of dichloromethane was cooled to 0 °C and *S*-camphorsulfonyl chloride (40 mg, 0.16 mmol, 1.2 equiv) was added. Stirring was continued for 2 h at 0 °C, and then 3 days at room temperature before water (10 ml) was added. The reaction mixture was diluted with CH_2Cl_2 (20 ml). The organic phase was washed with brine, dried over $MgSO_4$, and concentrated under vacuo. The product was purified by flash chromatography on silica gel (hexane/EA=2:1) to afford 9.5 mg of a white solid, along with recovered starting material (20 mg). R_f (hexane/EA 1:2)=0.24 (UV, Mostaine). δ_H (300 MHz, $CDCl_3$): 0.98 (s, CH_3–camphor, 3H), 1.21 (s, CH_3–camphor, 3H), 1.37–1.46 (s, CH_2-6′, 1H), 1.65–1.74 (m, CH_2-6′, 1H), 1.53 (d, J=6.6, CH_3-6, 3H), 1.91 (s, CH_2-3′, 1H), 1.97 (s, CH_2-3′, 1H), 2.01–2.17 (m, CH-4′, 1H), 2.35–2.51 (m, CH_2-5′, 2H), 2.53–2.77 (m, CH_2-3, 2H), 3.15 (d, J=15.0, CH_3-10′, 1H), 3.67 (d, J=15.0, CH_3-10′, 1H), 3.81–3.90 (m, CH_2-4, 1H), 3.94–4.02 (m, CH_2-4, 1H), 5.23–5.33 (m, CH-5, 1H), 7.24 (t, J=7.8, 1H, Ph), 7.42 (t, J=8.0, 2H, Ph), 7.65 (d, J=7.8, 2H, Ph); δ_C (75.5 MHz, $CDCl_3$): 16.7 (CH_3–camphor), 16.8 (CH_3–camphor), 19.9 (d, J=14.6, CH_3-7), 25.3 (CH_2-5′), 26.1 (d, J=23.5, CH_3-3), 27.0 (CH_2-6′), 42.6 (CH_2-3′), 43.0 (CH-4′), 44.9 (CH_2-4), 48.1 (C-7′), 48.7 (CH_2-10′), 58.2 (C-1′), 79.3 (d, J=27.6, CHOH-5), 97.7 (d, J=187.0, C-2), 120.3 (CH), 126.1 (CH), 129.3 (CH), 138.4 (C), 166.8 (d, J=22.2, CON-1), 214.1 (CO-2′); δ_F (188.3 MHz, $CDCl_3$): −149.8 (td, J=23.0, 10.8); ν_{max} (cm^{-1}, KBr pellet): 2960.9, 1749.4, 1704.1, 1497.3, 1358.2, 1168.1, 967.5, 920.8, 772.3, 506.5. Found: C, 60.55; H, 6.67; N, 2.98. $C_{22}H_{28}FNO_5S$ requires: C, 60.39; H, 6.45; N, 3.20.

Acknowledgements

We thank Dr. Diego Broggini and Dr. Sebastian Gischig for determining the crystal structures of compounds **3a** and **7**, Dr. Heinz Rüegger for assistance with the 2D NMR characterization of complexes **3**, and ETH for financial support (Ph.D. theses of M.P. and Y.L.).

References and notes

1. Hintermann, L.; Togni, A. *Angew. Chem., Int. Ed.* **2000**, *39*, 4359–4362.
2. Enders, D.; Hüttl, M. R. M. *Synlett* **2005**, 991–993.
3. Bernardi, L.; Jørgensen, K. A. *Chem. Commun.* **2005**, 1324–1326.
4. Hamashima, Y.; Suzuki, T.; Shimura, Y.; Shimizu, T.; Umebayashi, N.; Tamura, T.; Sasamoto, N.; Sodeoka, M. *Tetrahedron Lett.* **2005**, *46*, 1447–1450.
5. Shibata, N.; Kohno, J.; Takai, K.; Ishimaru, T.; Nakamura, S.; Toru, T.; Kanemasa, S. *Angew. Chem., Int. Ed.* **2005**, *44*, 4204–4207.
6. Steiner, D. D.; Mase, N.; Barbas, C. F., III. *Angew. Chem., Int. Ed.* **2005**, *44*, 3706–3710.
7. Ran Kim, H.; Young Kim, D. *Tetrahedron Lett.* **2005**, *46*, 3115–3117.
8. Beeson, T. D.; MacMillan, D. W. C. *J. Am. Chem. Soc.* **2005**, *127*, 8826–8828.
9. France, S.; Wheatherwax, A.; Lectka, T. *Eur. J. Org. Chem.* **2005**, 475–479.
10. Oestreich, M. *Angew. Chem., Int. Ed.* **2005**, *44*, 2324–2327.
11. Ibrahim, H.; Togni, A. *Chem. Commun.* **2004**, 1147–1155.
12. Ma, J.-A.; Cahard, D. *Chem. Rev.* **2004**, *104*, 6119–6146.
13. Seebach, D.; Beck, A. K.; Heckel, A. *Angew. Chem., Int. Ed.* **2001**, *40*, 92–138.
14. Mikami, K.; Terada, M. *Lewis Acids in Organic Synthesis*; Yamamoto, H., Ed.; Wiley-VCH: Weinheim, 2000; Vol. 2, pp 799–848.
15. (a) Hintermann, L.; Togni, A. *Helv. Chim. Acta* **2000**, *83*, 2425–2435; (b) Ibrahim, H.; Kleinbeck, F.; Togni, A. *Helv. Chim. Acta* **2004**, *87*, 605–610.
16. Frantz, R.; Hintermann, L.; Perseghini, M.; Broggini, D.; Togni, A. *Org. Lett.* **2003**, *5*, 1709–1712.
17. Toullec, P. Y.; Bonaccorsi, C.; Mezzetti, A.; Togni, A. *Proc. Natl. Acad. Sci. U.S.A.* **2004**, *101*, 5810–5814.
18. Jereb, M.; Togni, A. *Org. Lett.* **2005**, *7*, 4041–4043.
19. Piana, S.; Devillers, I.; Togni, A.; Röthlisberger, U. *Angew. Chem., Int. Ed.* **2002**, *41*, 979–982.
20. Shao, M.-Y.; Gau, H.-M. *Organometallics* **1998**, *17*, 4822–4827.
21. Shao, M.-Y.; Sheen, W.-S.; Gau, H.-M. *Inorg. Chim. Acta* **2001**, *314*, 105–110.
22. Haase, C.; Sarko, C. R.; DiMare, M. *J. Org. Chem.* **1995**, *60*, 1777–1787.
23. Gothelf, K. V.; Hazell, R. G.; Jørgensen, K. A. *J. Am. Chem. Soc.* **1995**, *117*, 4435–4436.
24. Gothelf, K. V.; Jørgensen, K. A. *J. Chem. Soc., Perkin Trans. 2* **1997**, 111–115.

25. Jensen, K. B.; Gothelf, K. V.; Hazell, R. G.; Jørgensen, K. A. *J. Org. Chem.* **1997**, *62*, 2471–2477.
26. Pichota, A.; Pregosin, P. S.; Valentini, M.; Wörle, M.; Seebach, D. *Angew. Chem., Int. Ed.* **2000**, *39*, 153–156.
27. Inoue, T.; Kitagawa, O.; Ochiai, O.; Shiro, M.; Taguchi, T. *Tetrahedron Lett.* **1995**, *36*, 9333–9336.
28. Seebach, D.; Plattner, D. A.; Beck, A. K.; Wang, Y. M. *Helv. Chim. Acta* **1992**, *75*, 2171–2209.
29. Hafner, A.; Duthaler, R. O.; Marti, R.; Rihs, G.; Rothe-Streit, P.; Schwarzenbach, F. *J. Am. Chem. Soc.* **1992**, *114*, 2321–2336.
30. Duthaler, R. O.; Hafner, A.; Alsters, P. L.; Bold, G.; Rihs, G.; Rothe-Streit, P.; Wyss, B. *Inorg. Chim. Acta* **1994**, *222*, 95–113.
31. Hintermann, L.; Broggini, D.; Togni, A. *Helv. Chim. Acta* **2002**, *85*, 1597–1612.
32. Sanger, A. R. *Inorg. Nucl. Chem. Lett.* **1973**, *9*, 351–354.
33. Hattori, K.; Yamada, A.; Kuroda, S.; Chiba, T.; Murata, M.; Sakane, K. *Bioorg. Med. Chem. Lett.* **2002**, *12*, 383–386.
34. Toullec, P. Y.; Devillers, I.; Frantz, R.; Togni, A. *Helv. Chim. Acta* **2004**, *87*, 2706–2711.
35. Ohkuma, T.; Noyori, R. *Comprehensive Asymmetric Catalysis*; Jacobsen, E. N., Pfaltz, A., Yamamoto, H., Eds.; Springer: Berlin, 2004; Supplement 1, pp 1–41, and references cited therein.